Original Article
Sodium iodide symporter expression driven by the survivin promoter enables radionuclide imaging and therapy for A549 non-small cell lung cancer

Zhen Zhao[*], Rui Huang[*], Huawei Cai, Bin Liu, Yu Zeng, Anren Kuang

Department of Nuclear Medicine, West China Hospital of Sichuan University, Chengdu, Sichuan Province, China. [*]Equal contributors.

Abstract: This study aimed to develop a gene expression targeting method specific for the imaging and therapy of non-small cell lung cancer A549 cells using an adenovirus vector containing the human sodium iodide symporter (NIS) gene driven by the survivin promoter. The recombinant adenovirus which contains the NIS gene and is driven by the survivin promoter, was name Ad-Sur-NIS, and transfected into A549 lung cancer cells and human normal dental pulp fibroblast DPF cells. NIS gene expression was evaluated using ^{125}I uptake and efflux assays. Additionally, the adenovirus was intratumorally injected into tumor-bearing mice for in vivo transfection; biodistribution studies and scintigraphic imaging were then performed. In vitro, the A549 cells exhibited perchlorate-sensitive iodide uptake following transfection with the Ad-Sur-NIS adenovirus that was 54-fold greater than that of the cells transfected with the Ad-Sur-GFP negative control. However, no significant iodide uptake was observed in the normal human DPF cells following adenovirus transfection. The clonogenic assays demonstrated that the Ad-Sur-NIS-transfected A549 cells were selectively killed by exposure to ^{131}I. In vivo, the Ad-Sur-NIS-transfected tumors also exhibited significant radio-iodine accumulation (16.96±2.99% ID/g at 2 h post-injection) with an effective half-life of 7.72±0.61 h. Moreover, the combination of Ad-Sur-NIS transfection and ^{131}I radionuclide therapy suppressed tumor growth and prolonged survival. These results indicate that the expression of NIS under the control of the survivin promoter may be used to achieve cancer-specific expression of NIS in A549 lung cancer cells, which may be a possible strategy for targeted cancer gene therapy.

Keywords: Sodium iodide symporter, survivin, adenovirus transfection, radioiodine therapy

Introduction

Lung cancer is the leading cause of cancer death among males worldwide and has surpassed breast cancer as the leading cause of cancer death among females in more developed countries [1]. Currently, patients with lung cancer are treated with various therapeutic options, such as surgery, chemotherapy, radiation therapy, or a combined modality approach [2]. However, the prognoses of patients suffering advanced lung cancer are still poor [3]. Consequently, the development of novel therapeutic strategies is indispensable.

The sodium iodide symporter (NIS) is an intrinsic membrane glycoprotein that takes up iodide into the cytosol from the extracellular fluid [4, 5]. Due to its expression in differentiated thy-roid cancer cells, NIS is the molecular basis for the diagnostic and therapeutic application of radioiodine, which has been successfully used in clinics for more than half a century [6]. In the last two decades, the understanding of the NIS has advanced rapidly, and NIS gene transfer makes it possible to image, monitor and treat tumors with appropriate radionuclides. The capacity of the NIS gene to induce radioiodine accumulation in non-thyroidal tumors has been investigated in a variety of tumor models by several groups including our own [6-11]. These data clearly demonstrate the potential of the NIS as a novel reporter and therapy gene for the imaging and treatment of non-thyroidal tumors.

In terms of ensuring tumor-specific radiation exposure, the application of tumor-specific pro-

moters offers the ability to induce NIS-selective expression in tumor cells. Several tumor-specific promoters are available for the targeting of individual cancers, such as the alpha fetoprotein (AFP) promoter for hepatocellular cancer [6, 7, 9], the prostate-specific antigen (PSA) promoter for prostate cancer [10], and the early growth response (EGR)-1 promoter for cervical cancer [11]. Although previous studies of promoters indicate that they are promising for carcinomas, specific promoters are required for specific tumors. Therefore, the identification of a more general tumor-related promoter for the regulation of NIS expression could be useful for expanding this strategy to the treatment of a wide variety of tumors.

Survivin, which is a member the apoptosis gene inhibitor family, has been reported to be expressed at high levels in cancerous tissues and absent in normal tissues [12, 13]. Clinical studies have indicated positive correlations between high survivin expression levels and advanced presentation, poor prognosis and increased resistance to therapy in cancer patients [14, 15]. Our previous work also convincingly demonstrated the proof of principle of the NIS gene under control of the survivin promoter in prostate tumors [8].

In this study, the survivin promoter was used to target NIS expression and induce radionuclide accumulation in non-small cell lung cancer A549 cells, and cell experiments, animal biodistribution, scintigraphic and therapeutic experiments were subsequently performed. The evaluation of the tumor-specific adenovirus efficacy was followed by the assessment of the NIS-mediated therapy response following the application of an additional therapeutic dose of ^{131}I.

Materials and methods

Cell culture

The human lung cancer cell line A549 was purchased from the American Type Culture Collection (ATCC, Rockville, MD, USA) and cultured in DMEM medium supplemented with 10% calf serum (Gibco, Carlsbad, CA, USA), 100 IU/ml penicillin, and 100 ng/ml streptomycin. The human normal dental pulp fibroblast (DPF) cell line was provided by Dr. Peng Li of the West China College of Stomatology, Sichuan

University and cultured as described previously [8]. Both cell lines were maintained at 37°C in a humidified atmosphere containing 5% CO_2.

Construction of the adenovirus and cell transfection

The replication-selective adenovirus Ad-Sur-NIS (1×10^9 PFU) carrying the NIS complementary DNA under the control of the survivin promoter and the replication-deficient adenovirus Ad-Sur-GFP (negative control) (1×10^9 PFU) carrying the GFP gene linked to the survivin promoter were developed as described previously [8]. For the in vitro transfection experiments, the A549 and DPF cells (1×10^6 cells per well in 6-well plates) were washed and incubated with 100 multiplicity of infection (MOI) per well of Ad-Sur-NIS or Ad-Sur-GFP for 2 h at 37°C and 5% CO_2. The media were replaced with fresh culture media, and virus-infected cells were further maintained for different times (24 h, 48 h or 72 h).

Analysis of the survivin promoter activity in vitro

To determine the transcriptional activation activity of the survivin promoter, we utilized the Dual-Luciferase Reporter Assay System (Promega, USA). The dual luciferase ratio was defined as previously described [8]. The pSV40-LUC vector (Promega, USA) containing the Simian Virus 40 (SV40) promoter was used as a positive control.

In vitro radioiodine uptake experiments

The cells were washed once with 1 ml of phosphate-buffered saline (PBS), and iodide uptake was then initiated by the addition of 1 ml of medium without serum containing 3.7 kBq of ^{125}I per well. To evaluate the time course of the iodide uptake, cells were incubated for 5, 10, 15, 20, 30, 60 and 90 min in the ^{125}I solution and then washed twice with ice-cold PBS and incubated for 20 min in 1 ml of ice-cold ethanol. The ethanol was then recovered, and the radioactivity was quantified (c.p.m.) using a gamma counter (No. 262 Factory, Xi'an, China). For the inhibition experiments, the cells were incubated with both 300 μM $KClO_4$ and ^{125}I for 30 min followed by the quantification of ^{125}I uptake as described above.

In vitro radioiodine efflux assay

A549 and DPF cells (1×10^6 cells per well) were seeded into 6-well plates, and incubated with Ad-Sur-NIS virus at MOI = 100 per well at 37°C and 5% CO_2 for 2 h. The medium was replaced with fresh culture medium, and the virus-infected cells were further maintained for 48 h. The cells were washed once with PBS, incubated in 1 ml of medium without serum containing 3.7 kBq of ^{125}I for 30 min, and washed twice with ice-cold PBS. Medium without serum (1 ml) was then added to each well and was replaced every 5 min for 30 min. The radioactivity in the medium was then quantified. After the removal of the final medium (at 30 min), the cells were solubilized for counting along with the previously collected medium samples. The total radioactivity at the initiation in the efflux study (100%) was calculated by adding the radioactivity of the final cells to the sum of the radioactivity of each medium [16].

Clonogenic assay

The clonogenic assay was performed by evaluating the cytotoxic effect of ^{131}I on the adenovirus-transfected cells. Briefly, the A549 and DPF cells transfected with Ad-Sur-NIS or Ad-Sur-GFP were seeded in 24-well tissue culture plates. Cells were incubated with 370 kBq of ^{131}I in 1 ml of RPMI-1640 medium with 0.5% fetal bovine serum. After 7 h incubation, cells were washed twice with PBS, trypsinized, and counted. Then, cells were plated in triplicate in six-well tissue culture plates (1000 cells per well) and incubated for 1 week at 37°C. Cells were then washed once with PBS and stained with crystal violet solution (2 g/l crystal violet, 4% formaldehyde, 20% ethanol). Colonies of >30 cells were counted, and the mean and s.d. of the number of colonies were determined. Results were expressed as the percentage of surviving cells, defined as the percentage of colonies obtained after treatment with [131]I.

Biodistribution of ^{125}I in the tumor-bearing mice

All of the protocols used in this report were approved by the Sichuan University Institutional Animal Care and Use Committee. A549 xenografts were established in 6-week-old Balb/c nude mice via the subcutaneous injection of 1×10^7 A549 cells into the flank region. The nude mice weighed 18-20 g. The experiments

began when tumors reached diameters of 8-10 mm. The Ad-Sur-NIS virus or the Ad-Sur-GFP virus (negative control) was injected into the tumors (1×10^9 PFU for each mouse). Two days later, radionuclide uptake was assessed via the intravenous injection of 370 kBq of [125]I. At 1, 2, 4, 8, and 24 h post-injection, the animals were sacrificed, and selected organs and tissues (i.e., the bone, muscle, heart, lung, liver, spleen, stomach, intestine, kidney, brain, and tumor) were dissected, weighed, and quantified for radioactivity. The results were expressed as the percentage of the injected dose per gram of tissue.

In vivo scintigraphic imaging of the tumor-bearing mice

Forty-eight hours after intratumoral injection of the adenovirus, the A549 tumor-bearing mice were injected with 18.5 MBq of [99mTc] via the tail vein. After 2 h, the animals were anesthetized with 2% isoflurane. The images were acquired using a Gamma SPECT system (Philips Medical Systems, Milpitas, CA). The SPECT scans were performed with a low-energy, high-resolution pinhole collimator with a field view of 12.5 cm and a reported resolution of 1 to 2 mm. Vertex views with at least 100,000 total counts per image were collected. The image acquisition times ranged from 2 to 3 min.

Immunohistochemical analysis of NIS protein expression

To detect the NIS expression, resected tumors from nude mice were fixed in 4% paraformaldehyde for 24 h. The samples were immunostained using a standard streptavidin-biotin labeling protocol as described previously [8].

In vivo ^{131}I therapy study

Animals with xenograft A549 tumors were injected with different adenoviruses followed by ^{131}I to evaluate the therapeutic effects. The experiments began when the tumors reached a size of 4-5 mm. After a 10-day pretreatment with thyroxine (Sigma-Aldrich, St Louis., MO; 5 mg/l) in their drinking water to reduce the radioiodide uptake by the thyroid gland, the animals were divided into the following four groups (n = 5): group one received a single intratumoral injection of 1×10^9 PFU of Ad-Sur-GFP; group two received 1×10^9 PFU of Ad-Sur-GFP and 111 MBq of [131]I 2 days later; group
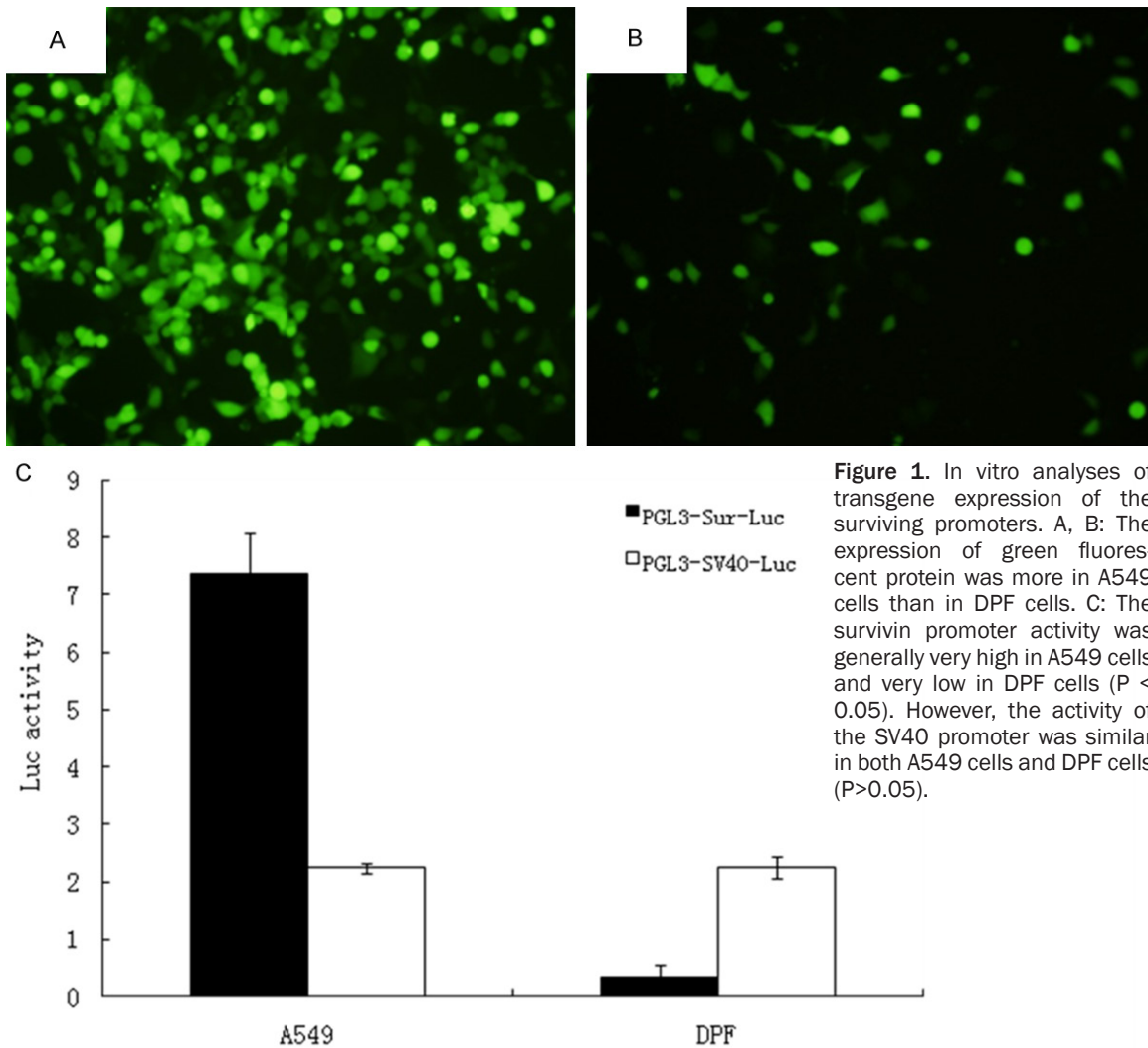
Figure 1. In vitro analyses of transgene expression of the surviving promoters. A, B: The expression of green fluorescent protein was more in A549 cells than in DPF cells. C: The survivin promoter activity was generally very high in A549 cells and very low in DPF cells (P < 0.05). However, the activity of the SV40 promoter was similar in both A549 cells and DPF cells (P>0.05).

three received 1×10^9 PFU of Ad-Sur-NIS only; and group four received both Ad-Sur-NIS and [131]I. The lengths and widths of the tumors were measured with a caliper at 5-day intervals following treatment. The tumor volumes were estimated using the following equation: $1/2 \times$ length $\times$ width^2 [8]. All mice were investigated over a total of 60 days and then euthanized.

Statistical analysis

All experiments were performed in triplicate. The SPSS version 17.0 software (SPSS Inc., Chicago, IL, USA) was applied for statistical analysis. The results were expressed as the mean ± standard deviation (SD). Differences between groups were analyzed by t-tests. The statistical significance of the survival curves was tested using the log-rank test. P < 0.05 was considered to be statistically significant.

Results

The activation of the survivin promoter in vitro

To assess the transcriptional activations of the survivin promoter and the SV40 promoter, we transfected both cancer (A549) and normal (DPF) cells with plasmids containing the luciferase gene under the control of either the survivin promoter (pSur-Luc) or the SV40 promoter (pSV40-Luc). The expression of green fluorescent protein was greater in the A549 cells than in the DPF cells (**Figure 1A**, **1B**). The activities of survivin promoter were generally high in the A549 cells while low in DPF cells (7.36±0.73 vs. 0.34±0.09, P < 0.05) (**Figure 1C**). However, the activities of the SV40 promoters were similar in the A549 cells and DPF cells (2.25±0.12 vs. 2.26±0.18, P>0.05) (**Figure 1C**). These data suggested that the survivin promoter was
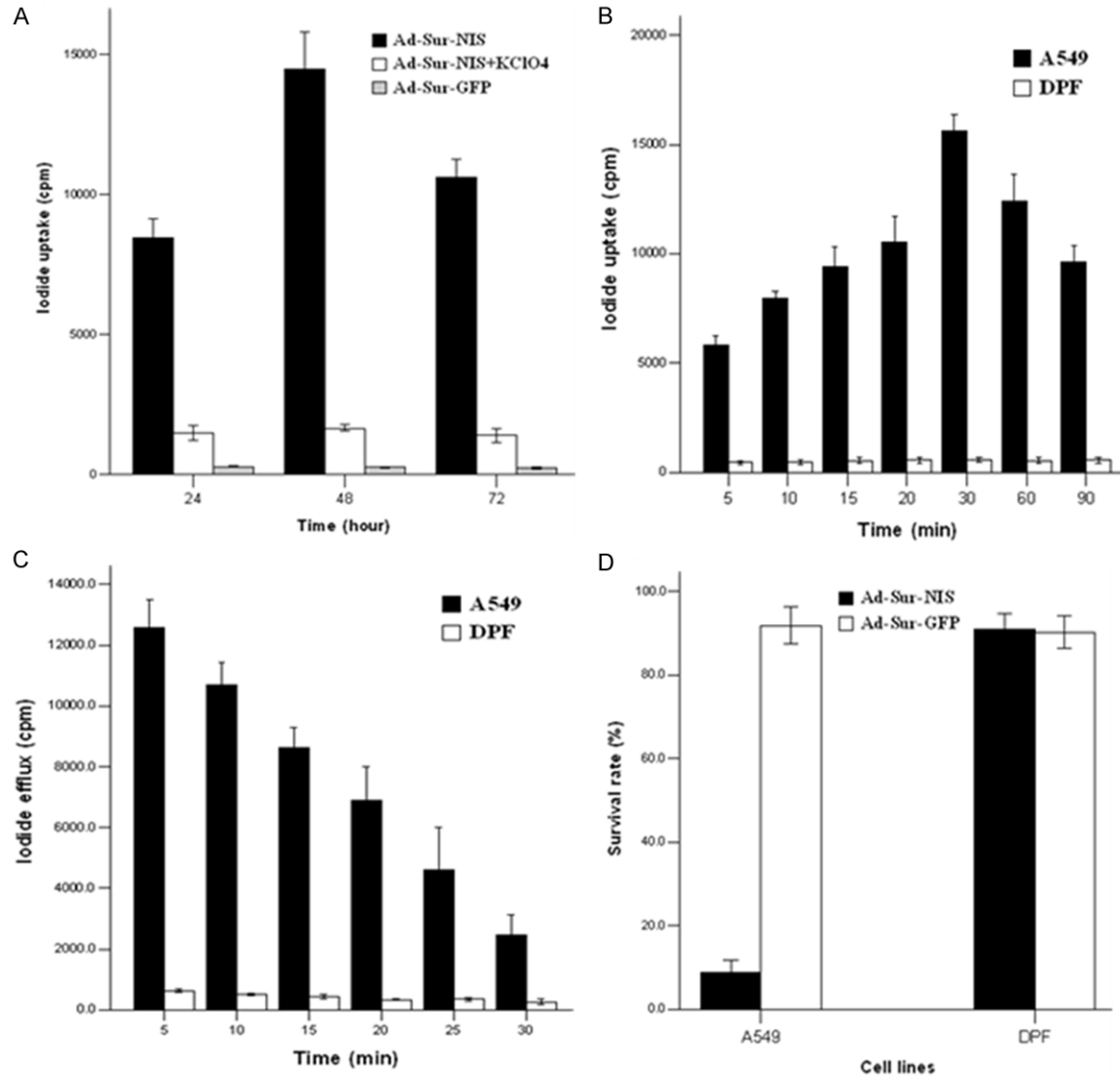
Figure 2. In vitro experiments. A, B: A549 cells were infected with 100 MOI Ad-Sur-NIS or Ad-Sur-GFP, and ^{125}I uptake was measured on hours 24, 48 and 72. Maximum iodide uptake was observed 48 hours following infection with Ad-Sur-NIS, when cells showed an 1.7-fold increase in uptake activity as compared with 24 hours after infection. A549 cells infected with Ad-Sur-NIS showed a 54-fold increase in perchlorate-sensitive ^{125}I accumulation. In contrast, no iodide uptake above background level was observed in A549 cells infected with Ad-Sur-GFP or in non-malignant cells (DPF) infected with Ad-Sur-NIS. Radioiodide uptake was rapidly increased, and maximized within 30 min in A549 infected with Ad-Sur-NIS. C: The effluxes of ^{125}I from A549 cells were rapid, with activity half lives ($T_{1/2}$) of 10 min. D: For evaluation of the therapeutic effect of ^{131}I in vitro, A549 cells infected with Ad-Sur-NIS were exposed to 370 kBq ^{131}I. While 90% of A549 cells infected with Ad-Sur-GFP or DPF cells infected with the adenovirus only survived, up to 90% of Ad-Sur-NIS-infected A549 cells were killed by radioiodine.

selectively active in the A549 cancer cells relative to the normal DPF cells.

Iodide influx and efflux studies in vitro

The transduction conditions for Ad-Sur-NIS were optimized in A549 tumor cells via the measurement of the perchlorate-sensitive iodide uptake activity. The perchlorate-sensitive iodide uptake activity was measured at

various time points after Ad-Sur-NIS infection (**Figure 2A**). The maximum iodide uptake activity was observed 48 hours following infection, at which point the A549 cells exhibited a 54-fold increase in perchlorate-sensitive ^{125}I accumulation compared with the A549 cells infected with the control virus (Ad-Sur-GFP) (P < 0.001) (**Figure 2A**). This uptake was inhibited by potassium perchlorate (**Figure 2A**), which is a potent inhibitor of active iodide transport,

Table 1. Biodistribution of ^{125}I in mice with Ad-Sur-NIS injected A549 xenografts (% ID/g tissue; mean and SD after intravenous injection)

Organ	1 h	2 h	4 h	8 h	24 h
Stomach	18.58±3.61	15.31±3.37	11.19±1.06	6.41±1.18	0.98±0.20
Tumor	12.06±2.31	16.96±2.99	14.63±3.41	7.92±2.35	1.37±0.51
Heart	4.47±0.74	3.63±1.13	2.81±1.25	1.65±1.06	0.32±0.15
Liver	2.60±0.50	2.15±0.48	0.78±0.21	0.77±0.13	0.17±0.07
Spleen	2.57±0.38	2.09±0.23	1.31±0.42	1.29±0.55	0.10±0.02
Lung	3.45±0.80	2.92±0.62	2.11±0.20	1.04±0.20	0.16±0.09
Kidney	4.38±1.05	3.85±0.90	2.09±0.67	1.45±0.53	0.16±0.04
Bone	1.32±0.41	1.07±0.24	0.85±0.18	0.40±0.12	0.10±0.07
Intestine	2.42±0.50	1.97±0.52	1.31±0.49	0.67±0.25	0.13±0.05
Muscle	0.91±0.18	0.70±0.11	0.54±0.09	0.30±0.07	0.09±0.02
Brain	0.23±0.04	0.14±0.04	0.16±0.02	0.07±0.02	0.05±0.01

confirming that iodide uptake was essentially dependent on NIS expression. Iodide uptake increased within 30 min due to the incubation of the Ad-Sur-NIS-infected A549 cells at different times with 3.7 kBq of ^{125}I (**Figure 2B**). The tumor specificity of Ad-Sur-NIS was confirmed via the infection of non-malignant control (DPF) cells that did not express survivin and exhibited a lack of iodide uptake activity (**Figure 2B**). In the radioiodine efflux study, 50.73±1.84% of the total radioiodine that accumulated in cells was washed out within the first 10 min, which corresponded to a ^{125}I half-life within the cells of approximately 10 min (**Figure 2C**).

In vitro clonogenic assay

To evaluate the therapeutic potential of ^{131}I in lung cancer cells (A549) using Ad-Sur-NIS infection in vitro, a clonogenic assay was performed with 370 kBq of ^{131}I (**Figure 2D**). Following exposure to ^{131}I, only 8.7±2.5% of the A549 cells infected with Ad-Sur-NIS survived, and 90.9±3.2% of the A549 cells infected with Ad-Sur-GFP survived (P < 0.001). No significant cell death was observed in either the Ad-Sur-NIS or Ad-Sur-GFP infected DPF cells treated with ^{131}I; specifically, 91.8±3.8% and 90.2± 3.4% of the cells were recovered, respectively. These results demonstrated that the coupling Ad-Sur-NIS infection and ^{131}I treatment efficiently and specifically led to cancer cell death in vitro.

^{125}I biodistribution studies in the tumor-bearing mice

Complete data on the ^{125}I biodistributions are provided in **Table 1**. In the Ad-Sur-NIS-tran-

sfected A549 tumors, the maximum activity levels per gram of tissue were 16.96± 2.99% ID/g, were reached at 2 h, and exhibited mean effective half-life of 7.72± 0.61 h. The negative control tumors infected with Ad-Sur-GFP accumulated 0.96± 0.21% ID/g at 1 h, 0.73± 0.14% ID/g at 2 h, 0.52± 0.08% ID/g at 4 h, 0.34± 0.06% ID/g at 8 h, and 0.09±0.02% ID/g at 24 h. The tumors infected with Ad-Sur-NIS exhibited as much as a 33-fold increase in iodide uptake activity at 2 h compared with the tumors infected with Ad-Sur-GFP. These data indicate that the infection of tumors with the Ad-Sur-NIS virus led to the selective uptake of ^{125}I in vivo.

^{99m}Tc scintigraphy in vivo

Because NIS mediates ^{99m}Tc uptake in specific tissues, scintigraphy was performed on the tumor-bearing mice to evaluate the adenovirus transfections in vivo via ^{99m}Tc imaging (**Figure 3A**, **3B**). Although no specific pertechnetate accumulation was detected in the A549 tumors after infection with Ad-Sur-GFP (**Figure 3B**), the Ad-Sur-NIS-infected A549 tumors exhibited a significant uptake of ^{99m}Tc (**Figure 3A**). In addition to tumor uptake, significant pertechnetate accumulation was observed in the tissues that physiologically express NIS, including the stomach and thyroid, and in the tissues involved in pertechnetate elimination (bladder).

Immunohistochemical analysis of NIS expression in the A549 xenografts

For the in vivo experiments, expressions of the NIS protein in the tumors were characterized by immunohistochemical staining. The tumors injected with adenovirus were specifically labeled with anti-NIS antibodies. The analysis revealed a staining pattern that involved areas of NIS-specific immunoreactivity in the tumors following the intratumoral application of Ad-Sur-NIS (**Figure 3C**). In contrast, the tumors infected with Ad-Sur-GFP (control) exhibited no NIS-specific immunoreactivity (**Figure 3D**).
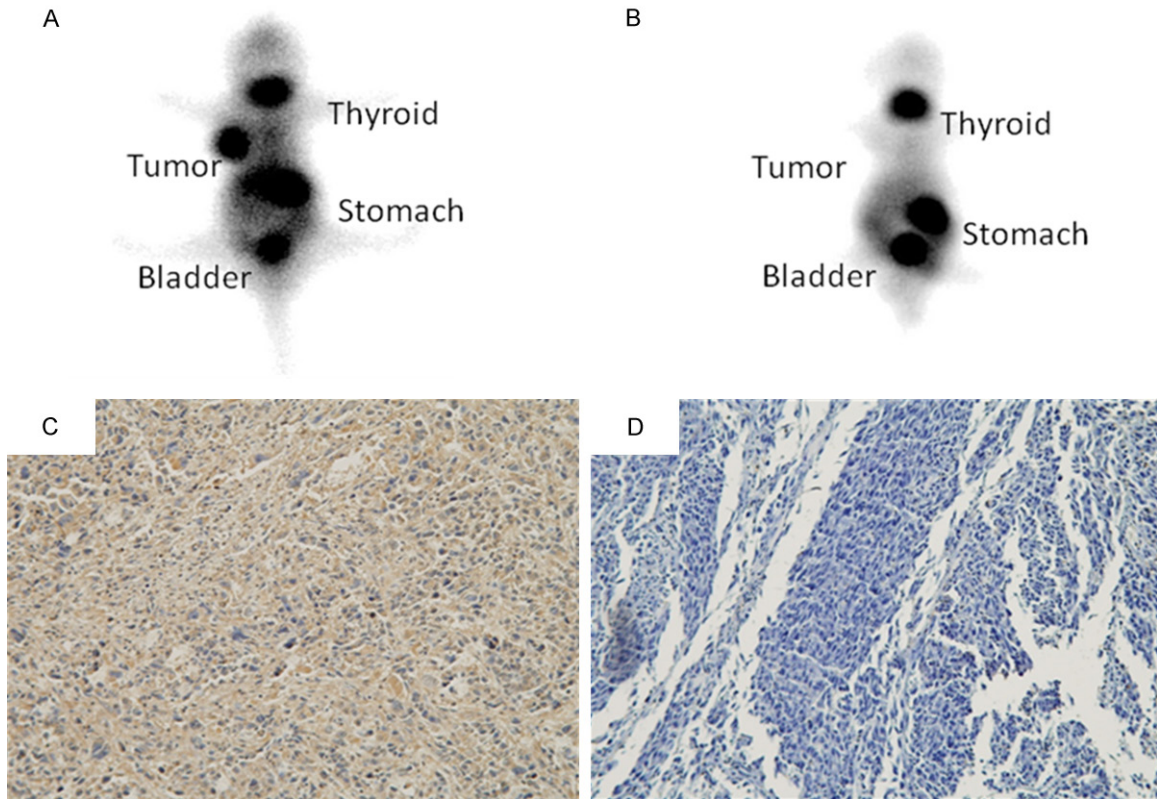
Figure 3. The ^{99m}Tc scintigraphic images and immunohistochemical staining. A, B: Mice harboring A549 xenograft tumors infected with either Ad-Sur-NIS or Ad-Sur-GFP were imaged with a pinhole collimator 2 h after injection of 18.5 MBq ^{99m}Tc. The Ad-Sur-NIS-infected tumor was clearly visible, with an intensity comparable to that of the thyroid or the bladder. The Ad-Sur-GFP infected tumor was not visible using ^{99m}Tc imaging. C: Immunohistochemical staining of A549 tumors infected with Ad-Sur-NIS showed NIS-specific immunoreactivity (×200). D: In contrast, A549 tumors infected with Ad-Sur-GFP did not reveal NIS-specific immunoreactivity (×200).

NIS transfection improved the radionuclide therapy effect in vivo

The tumors in the animals that received both Ad-Sur-GFP and 111 MBq ^{131}I, those that received only the Ad-Sur-GFP virus, and those that received only the Ad-Sur-NIS virus continued to grow until the end of the experiment, which demonstrated the lack of a therapeutic effect (**Figure 4A**, **4B**). Radionuclide therapy in the mice that were injected with Ad-Sur-NIS and 111 MBq ^{131}I elicited a strongly enhanced therapeutic effect as demonstrated by significantly delayed tumor growth and extensively prolonged survival (P < 0.001) (**Figure 4A**, **4B**). These results suggest that the expression of NIS in combination with treatment with a therapeutic dose of ^{131}I may prove to be a successful strategy for reducing tumor growth in vivo.

Discussion

The applications of NIS as a reporter and suicide gene for molecular imaging and targeted

therapy, have been demonstrated in many studies. Non-invasive imaging of NIS gene transfer in non-thyroidal tumors with gamma cameras, positron emission tomography and cerenkov luminescence imaging have been demonstrated to be safe and efficient [9, 16-20]. NIS also mediates the cellular accumulation of radionuclides, such as ^{131}I, ^{186}Re, ^{188}Re and ^{211}At, which are used for tumor therapy [21-26].

The use of the promoter-specific driving of NIS in target tissues has been adopted in cancer gene therapy in animal experimental models [6-11]. Many tumor-specific promoters have exhibited the capacity feasible and safely mediate NIS gene therapy. In our previous studies, we reported hepatoma-specific NIS expression via the application of the AFP promoter [7]. In contrast to single cancer-specific targeting promoters, the survivin promoter is multicancer-specific and thus has the potential to extend the scope of gene-based therapy [12, 13]. An adenovirus vector carrying the NIS gene under
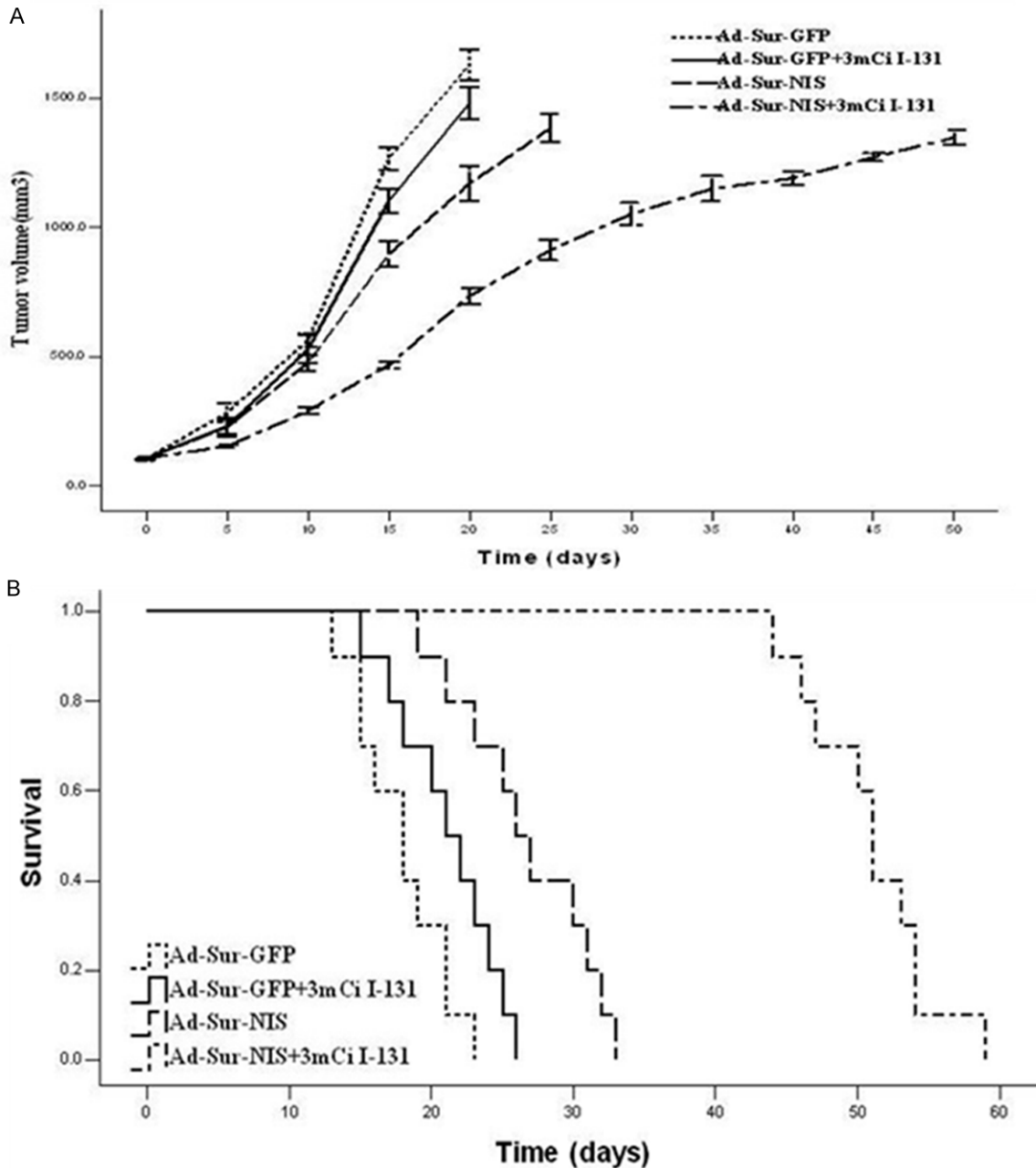
Figure 4. Therapeutic effects of Ad-Sur-NIS infection in combination with ^{131}I treatment in A549 xenografts. A, B: Radioiodine therapy studies showed excessive tumor growth of control groups treated with Ad-Sur-GFP and 111 MBq ^{131}I, or only Ad-Sur-GFP, or only Ad-Sur-NIS, no therapeutic effect was observed. Intratumoral injection of Ad-Sur-NIS followed by additional application of 111 MBq ^{131}I resulted in strongly enhanced therapeutic effect, as seen by significantly delayed tumor growth and prolonged survival (P < 0.001).

control of the survivin promoter was able to induce tumor-specific functional NIS expression in survivin-positive PC3 prostate cancer cells at a level that was sufficiently high to allow for cytoreductive responses of ^{131}I accumulation both in vitro and in vivo following local application [8]. This successful experience exemplifies our efforts toward the application of Ad-Sur-NIS to lung cancer, which has a relatively high incidence and mortality among East Asians [27]. Therefore, the survivin promoter was used to induce NIS expression and radionuclide accumulation in A549 lung cancer cells in the present study.

Functional NIS protein expression following adenoviral NIS gene transfer was confirmed via the in vitro measurement of radioiodine uptake. Ad-Sur-NIS exhibited high transduction efficiency and tumor selectivity, and the maximal transduction efficiency was obtained at 48 h after virus application. The expression of NIS in A549 cells via the Ad-Sur-NIS virus increased the accumulation of perchlorate-sensitive iodide by up to 54-fold over that of negative control Ad-Sur-GFP infected cells. Furthermore, no significant iodide uptake was observed in the Ad-Sur-NIS-infected non-malignant DPF cells, which indicated that the virus selectively targeted A549 lung cancer cells. The capability to concentrate high levels of radioiodine resulted in a significant therapeutic effect of ^{131}I in A549 lung cancer cells in vitro as confirmed by the clonogenic assay.

We further investigated the in vivo application of Ad-Sur-NIS for the delivery of the NIS gene to lung cancer xenografts. Scintigraphy and biodistribution studies confirmed that the specific accumulation of the radionuclide also occurred in the Ad-Sur-NIS-infected A549 tumors in vivo. At 48 h after the intratumoral injection of Ad-Sur-NIS, a tumor-specific ^{125}I accumulation of 16.96±2.99% ID/g was observed at 2 h post-injection, and the effective half-life was 7.72± 0.61 h. In our previous study, Ad-Sur-NIS-infected PC3 xenografts accumulated 13.3± 2.85% ID/g ^{125}I at 2 h post-injection with an effective half-life of 3.1 h [8]. Notably, the A549 tumors accumulated a greater amount of radioiodine and exhibited a longer effective half-life compared with the PC3 tumors, which indicated that the detailed iodide retention mechanisms differed between these two cell types, and this difference in mechanisms would be our interest in the future. The therapeutic results demonstrated that the intratumoral injection of Ad-Sur-NIS followed by the additional application of 111 MBq ^{131}I induced a strong stimulation of the therapeutic effects of the radioactive iodide that included an extensively delayed tumor growth and a prolonged survival compared with the 111 MBq ^{131}I and Ad-Sur-GFP, Ad-Sur-GFP alone, and Ad-Sur-NIS alone treatments (P < 0.001). NIS-mediated radionuclide therapy may also be more effective due to a substantial bystander effect, which may compensate for limited viral spread in the tumor and reduce the level of transduction efficiency [6]. Additional cell killing may have occurred due to radiological crossfire; i.e., ^{131}I decay produces β-particles that damage cellular proteins and nucleic acids [28, 29].

The treatment efficacy of the radiotherapy is strictly dependent on the biological half-life of the radionuclide in the tumors [30]. The main problem concerns the short retention time of radioiodine in tumor cells [31]. In our radioiodine efflux assay, only 5.33±1.03% of radionuclide activity remained at 30 min, and in our biodistribution study, the percentage ^{125}I uptake by the Ad-Sur-NIS-infected A549 tumors fell from 16.96±2.99% ID/g at 2 h post-injection to 1.37±0.51% ID/g at 24 h. For molecular imaging purposes, this is not a substantial issue because optimal imaging times can be determined, but in terms of radionuclide therapy, fast washout remains a major problem [32]. Strategies to improve therapeutic response, such as prolonging the retention time and restoring/up-regulating NIS expression [26], are under investigation. In our previous work, thyroid-specific transcription factor (TTF)-1 and Pax-8 gene transcriptions were able to induce iodide uptake and specifically prolong the iodide retention time by promoting the expressions of thyroperoxidase (TPO) and thyroglobulin (Tg) proteins in cancer cells [33, 34]. Retinoic acid, dexamethasone and 5-azacytidine can increase radioiodine uptake via the up-regulation of NIS expression [35-37].

It is worth nothing that stomach indicated ^{131}I, uptake as high as tumor at 1 h in our biodistribution, which may be caused by the relative high expression of NIS in this organ. Endogenous NIS in stomach induces transient radioactive iodine; the retention time is much shorter than in tumors in longer time evaluation throughout 2 h to 24 h, which is consistent with other studies [32, 38, 39]. In clinic cases, there is no significant increased gastrointestinal risk observed in thyroid cancer patients with oral ^{131}I treatments, a simple routine of having patients drink gastric mucosal protective drugs could minimize potential risk of stomach [8].

In conclusion, our study clearly demonstrates that the tumor-specific expression of the NIS gene under the control of the survivin promoter allows for targeted NIS-mediated, imaging-guided radionuclide therapy for A549 lung tumors,

which proves the potential of this system for clinical application.

Disclosure of conflict of interest

None.

Address correspondence to: Anren Kuang, Department of Nuclear Medicine, West China Hospital of Sichuan University, 37 Guoxue Alley, Chengdu 610041, Sichuan Province, China. Tel: +86-18980601582; Fax: +86-28-85422155; E-mail: kuanganren@263.net

References

[1] Torre LA, Bray F, Siegel RL, Ferlay J, Lortet-Tieulent J, Jemal A. Global cancer statistics, 2012. CA Cancer J Clin 2015; 65: 87-108.

[2] Farhat FS, Houhou W. Targeted therapies in non-small cell lung carcinoma: what have we achieved so far? Ther Adv Med Oncol 2013; 5: 249-70.

[3] Griffioen GH, Toguri D, Dahele M, Warner A, de Haan PF, Rodrigues GB, Slotman BJ, Yaremko BP, Senan S, Palma DA. Radical treatment of synchronous oligometastatic non-small cell lung carcinoma (NSCLC): patient outcomes and prognostic factors. Lung Cancer 2013; 82: 95-102.

[4] Filetti S, Bidart JM, Arturi F, Caillou B, Russo D, Schlumberger M. Sodium/iodide symporter: a key transport system in thyroid cancer cell metabolism. Eur J Endocrinol 1999; 141: 443-57.

[5] Nilsson M. Molecular and cellular mechanisms of transepithelial iodide transport in the thyroid. Biofactors 1999; 10: 277-85.

[6] Grünwald GK, Klutz K, Willhauck MJ, Schwenk N, Senekowitsch-Schmidtke R, Schwaiger M, Zach C, Göke B, Holm PS, Spitzweg C. Sodium iodide symporter (NIS)-mediated radiovirotherapy of hepatocellular cancer using a conditionally replicating adenovirus. Gene Ther 2013; 20: 625-33.

[7] Ma XJ, Huang R, Kuang AR. AFP promoter enhancer increased specific expression of the human sodium iodide symporter (hNIS) for targeted radioiodine therapy of hepatocellular carcinoma. Cancer Invest 2009; 27: 673-81.

[8] Huang R, Zhao Z, Ma X, Li S, Gong R, Kuang A. Targeting of tumor radioiodine therapy by expression of the sodium iodide symporter under control of the survivin promoter. Cancer Gene Ther 2011; 18: 144-52.

[9] Grünwald GK, Vetter A, Klutz K, Willhauck MJ, Schwenk N, Senekowitsch-Schmidtke R, Schwaiger M, Zach C, Wagner E, Göke B, Holm PS, Ogris M, Spitzweg C. Systemic image-guided liver cancer radiovirotherapy using dendrimer-coated adenovirus encoding the sodium iodide symporter as theranostic gene. J Nucl Med 2013; 54: 1450-7.

[10] Willhauck MJ, Samani BR, Wolf I, Senekowitsch-Schmidtke R, Stark HJ, Meyer GJ, Knapp WH, Göke B, Morris JC, Spitzweg C. The potential of 211 Astatine for NIS-mediated radionuclide therapy in prostate cancer. Eur J Nucl Med Mol Imaging 2008; 35: 1272-81.

[11] Tang J, Wang X, Xu Y, Shi Y, Liu Z, Yang Y. Sodium-iodine symporter gene expression controlled by the EGR-1 promoter: biodistribution, imaging and in vitro radionuclide therapy with Na(131)I. Technol Cancer Res Treat 2015; 14: 61-9.

[12] Jaiswal PK, Goel A, Mittal RD. Survivin: a molecular biomarker in cancer. Indian J Med Res 2015; 141: 389-97.

[13] Huang J, Lyu H, Wang J, Liu B. MicroRNA regulation and therapeutic targeting of survivin in cancer. Am J Cancer Res 2015; 15: 20-31.

[14] Singh N, Krishnakumar S, Kanwar RK, Cheung CH, Kanwar JR. Clinical aspects for survivin: a crucial molecule for targeting drug-resistant cancers. Drug Discov Today 2015; 20: 578-87.

[15] Khan S, Ferguson Bennit H, Asuncion Valenzuela MM, Turay D, Diaz Osterman CJ, Moyron RB, Esebanmen GE, Ashok A, Wall NR. Localization and upregulation of survivin in cancer health disparities: a clinical perspective. Biologics 2015; 9: 57-67.

[16] Kim KI, Lee YJ, Lee TS, Song I, Cheon GJ, Lim SM, Chung JK, Kang JH. In vitro radionuclide therapy and in vivo scintigraphic imaging of alpha-fetoprotein-producing hepatocellular carcinoma by targeted sodium iodide symporter gene expression. Nucl Med Mol Imaging 2013; 47: 1-8.

[17] Wolfs E, Holvoet B, Gijsbers R, Casteels C, Roberts SJ, Struys T, Maris M, Ibrahimi A, Debyser Z, Van Laere K, Verfaillie CM, Deroose CM. Optimization of multimodal imaging of mesenchymal stem cells using the human sodium iodide symporter for PET and Cerenkov luminescence imaging. PLoS One 2014; 9: e94833.

[18] Lee HW, Yoon SY, Singh TD, Choi YJ, Lee HJ, Park JY, Jeong SY, Lee SW, Ha JH, Ahn BC, Jeon YH, Lee J. Tracking of dendritic cell migration into lymph nodes using molecular imaging with sodium iodide symporter and enhanced firefly luciferase genes. Sci Rep 2015; 5: 9865.

[19] Hickey RD, Mao SA, Amiot B, Suksanpaisan L, Miller A, Nace R, Glorioso J, O'Connor MK, Peng KW, Ikeda Y, Russell SJ, Nyberg SL. Noninvasive 3-dimensional imaging of liver regeneration in a mouse model of hereditary tyrosin-

emia type 1 using the sodium iodide symporter gene. Liver Transp 2015; 21: 442-53.

[20] Barton KN, Stricker H, Brown SL, Elshaikh M, Aref I, Lu M, Pegg J, Zhang Y, Karvelis KC, Siddiqui F, Kim JH, Freytag SO, Movsas B. Phase I study of noninvasive imaging of adenovirus-mediated gene expression in the human prostate. Mol Ther 2008; 16: 1761-9.

[21] Knoop K, Schwenk N, Schmohl K, Müller A, Zach C, Cyran C, Carlsen J, Böning G, Bartenstein P, Göke B, Wagner E, Nelson PJ, Spitzweg C. Mesenchymal stem cell-mediated, tumor stroma-targeted radioiodine therapy of metastatic colon cancer using the sodium iodide symporter as theranostic gene. J Nucl Med 2015; 56: 600-6.

[22] Kotzerke J, Wendisch M, Freudenberg R, Runge R, Oehme L, Meyer GJ, Kunz-Schughart LA, Wunderlich G. Sodium-iodide symporter positive cells after intracellular uptake of Tc-99m versus alpha-emitter At-211 reduction of clonogenic survival and characterization of DNA damage. Nuklearmedizin 2012; 51: 170-8.

[23] Guo R, Zhang M, Xi Y, Ma Y, Liang S, Shi S, Miao Y, Li B. Theranostic studies of human sodium iodide symporter imaging and therapy using Re-188: a human glioma study in mice. PLoS One 2014; 9: e102011.

[24] Knoop K, Schwenk N, Dolp P, Willhauck MJ, Zischek C, Zach C, Hacker M, Göke B, Wagner E, Nelson PJ, Spitzweg C. Stromal targeting of sodium iodide symporter using mesenchymal stem cells allows enhanced imaging and therapy of hepatocellular carcinoma. Hum Gene Ther 2013; 24: 306-16.

[25] Barton KN, Stricker H, Elshaikh MA, Pegg J, Cheng J, Zhang Y, Karvelis KC, Lu M, Movsas B, Freytag SO. Feasibility of adenovirus-mediated hNIS gene transfer and (131)I radioiodine therapy as a definitive treatment for localized prostate cancer. Mol Ther 2011; 19: 1353-9.

[26] Ahn BC. Sodium iodide symporter for nuclear molecular imaging and gene therapy: from bedside to bench and back. Theranostics 2012; 2: 392-402.

[27] Zhang Q, Jin H, Wang L, Xin B, Zhang J, Zhou Y, Sheng S. Lung cancer risk and genetic variants in East Asians: a meta-analysis. Tumour Biol 2014; 35: 5173-9.

[28] Boswell CA, Brechbiel MW. Development of radioimmunotherapeutic and diagnostic antibodies: an inside-out view. Nucl Med Biol 2007; 34: 757-78.

[29] Hutzen B, Pierson CR, Russell SJ, Galanis E, Raffel C, Studebaker AW. Treatment of medulloblastoma using an oncolytic measles virus encoding the thyroidal sodium iodide symporter shows enhanced efficacy with radioiodine. BMC Cancer 2012; 12: 508.

[30] Micali S, Bulotta S, Puppin C, Territo A, Navarra M, Bianchi G, Damante G, Filetti S, Russo D. Sodium iodide symporter (NIS) in extrathyroidal malignancies: focus on breast and urological cancer. BMC Cancer 2014; 14: 303.

[31] Chen L, Altmann A, Mier W, Eskerski H, Leotta K, Guo L, Zhu R, Haberkorn U. Radioiodine therapy of hepatoma using targeted transfer of the human sodium/iodide symporter gene. J Nucl Med 2006; 47: 854-62.

[32] Schipper ML, Riese CG, Seitz S, Weber A, Béhé M, Schurrat T, Schramm N, Keil B, Alfke H, Behr TM. Efficacy of 99mTc pertechnetate and 131I radioisotope therapy in sodium/iodide symporter (NIS)-expressing neuroendocrine tumors in vivo. Eur J Nucl Med Mol Imaging 2007; 34: 638-50.

[33] Mu D, Huang R, Ma X, Li S, Kuang A. Radioiodine therapy of thyroid carcinoma following Pax-8 gene transfer. Gene Ther 2012; 19: 435-42.

[34] Mu D, Huang R, Li S, Ma X, Lou C, Kuang A. Combining transfer of TTF-1 and Pax-8 gene: a potentialstrategy to promote radioiodine therapy of thyroid carcinoma. Cancer Gene Ther 2012; 19: 402-11.

[35] Tang M, Hou YL, Kang QQ, Chen XY, Duan LQ, Shu J, Li SL, Hu XL, Peng ZP. All-trans-retinoic acid promotes iodine uptake via up-regulating the sodium iodide symporter in medullary thyroid cancer stem cells. Asian Pac J Cancer Prev 2014; 15: 1859-62.

[36] Willhauck MJ, Sharif-Samani B, Senekowitsch-Schmidtke R, Wunderlich N, Göke B, Morris JC, Spitzweg C. Functional sodium iodide symporter expression in breast cancer xenografts in vivo after systemic treatment with retinoic acid and dexamethasone. Breast Cancer Res Treat 2008; 109: 263-72.

[37] Li W, Venkataraman GM, Ain KB. Protein synthesis inhibitors, in synergy with 5-azacytidine, restore sodium/iodide symporter gene expression in human thyroid adenoma cell line, KAK-1, suggesting trans-active transcriptional repressor. J Clin Endocrinol Metab 2007; 92: 1080-7.

[38] Kogai T, Brent GA. The sodium iodide symporter (NIS): regulation and approaches to targeting for cancer therapeutics. Pharmacol Ther 2012; 135: 355-70.

[39] Kim SH, Chung HK, Kang JH, Kim KI, Jeon YH, Jin YN, Yun CO, Chung JK. Tumor-targeted radionuclide imaging and therapy based on human sodium iodide symporter gene driven by a modified telomerase reverse transcriptase promoter. Hum Gene Ther 2008; 19: 951-7.